Springer

Journal of
Mechanical
Science and
Technology

Journal of Mechanical Science and Technology 22 (2008) 429~439

www.springerlink.com/content/1738-494x

Buckling analysis of multi-walled carbon nanotubes under combined loading considering the effect of small length scale

A. Ghorbanpour Arani*, R. Rahmani, A. Arefmanesh and S. Golabi

Department of Mechanical Engineering, Faculty of Engineering, University of Kashan, Kashan, I.R. of Iran.

(Manuscript Received April 16, 2007; Revised October 27, 2007; Accepted October 27, 2007)

Abstract

The torsional and axially compressed buckling of an individual embedded multi-walled carbon nanotube (MWNTs) subjected to an internal and/or external radial pressure was investigated in this study. The emphasis is placed on new physical phenomena which are due to both the small length scale and the surrounding elastic medium. Multiwall carbon nanotubes which are considered in this study are classified into three categories based on the radius to thickness ratio, namely, thin, thick, and almost solid. Explicit formulas are derived for the van der Waals (vdW) interaction between any two layers of an MWNT based on the continuum cylindrical shell model. In most of the previous studies, the vdW interaction between two adjacent layers was considered only and the vdW interaction among other layers was neglected. Moreover, in these works, the vdW interaction coefficient was treated as a constant that was independent of the radii of the tubes. However, in the present model the vdW interaction coefficients are considered to be dependent on the change of interlayer spacing and the radii of the tubes. The effect of the small length scale is also considered in the present formulation. The results show that there is a unique buckling mode (*m,n*) corresponding to the critical shear stress. This result is obviously different from what is expected for the pure axially compressed buckling of an individual multi-walled carbon nanotube.

Keywords: Carbon nanotubes; Buckling; van der Waals interaction; Continuum shell model; Small length scale; Elastic medium

1. Introduction

Carbon nanotubes, which were discovered by Sumio Iijima [1], have widespread applications in different fields such as chemistry, physics, engineering, material science and reinforced composite structures. It is commonly believed in the scientific community that nanotechnology will spark a series of industrial revolutions in the following decades. The discovery of carbon nanotubes has been a very significant breakthrough that has accelerated further developments in the field of nanotechnology. Carbon nanotubes (CNTs) are among the most promising new materials and are expected to play a pivotal role in the future of nanotechnology. Due to the difficulties in experimental characterization of nanotubes, mechanical responses of carbon nanotubes are mainly investigated through numerical simulations using atomistic or continuum models.

Abrupt changes in the physical and mechanical properties of single-walled carbon nanotubes (SWNTs) and MWNTs are observed when the applied load and pressure reach a critical value. To investigate this issue, nonlocal continuum models have been proposed to extend the classical continuum approach to smaller length scales by incorporating information regarding the behavior of material microstructure while retaining most of the advantages of the classical model. The theory of nonlocal continuum mechanics was first introduced by Eringen in his work on nonlocal elasticity [2]. In this theory, contrary to the classical continuum mechanics, the stress at a point is considered to be a function of the strain at

*Corresponding author. Tel.: +98 361 557 0065, Fax.: +98 361 555 9930
E-mail address: aghorban@kashanu.ac.ir
DOI 10.1007/s12206-007-1045-2

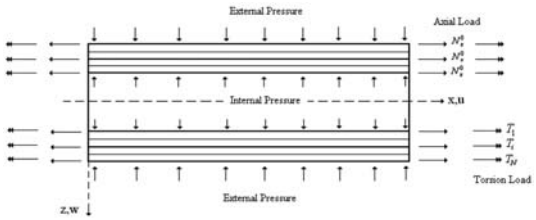

Fig. 1. A multi-walled carbon nanotube in an infinite elastic medium with loading configuration.

all the points throughout the body. Moreover, the effect of radial constraint from the surrounding infinite elastic medium, which is dependent on the dimensions of MWNTs, is taken into account. This effect represents an initial interaction pressure between, known as the external radial pressure, the outermost layer of the multi-walled carbon nanotube and its surrounding elastic medium. Combined loading and lateral pressure for a multi-walled carbon nanotube is shown in Fig. 1.

The critical axial stress and strain increase for different filling molecules (about 10% at low density and up to 40% for filling molecules at high density). As stated before, the effect of filling molecules can be modeled approximately by an internal radial pressure. In most of the previous studies, to model vdW forces, a linear relationship between the vdW force and the normal deflection was assumed. A simple relationship for the vdW interaction coefficient has been obtained based on this assumption (C= 320 $erg/c\,m^2/0.16\,d^2$, d=0.142 nm) [3]. The linear model does not take into account the effect of the radius of the CNT on the vdW interaction coefficient. In this study, basic equations for a cylindrical shell under uniform external and/or internal radial pressure, torsion, and axial loading are formulated based on the theory of nonlocal elasticity.

2. Basic equations

2.1 Governing equations

Consider a multi-walled CNT, consisting of two or more single CNTs, of radius R_i, thickness *h*, modulus of elasticity *E*, and Poisson's ratio *v.* An internal or an external radial pressure and also the pressure caused by vdW interaction are applied to the tube. It is assumed that there is no slip between the layers. The membrane strains, the membrane forces prior to buckling, and the membrane forces due to buckling under these circumstance are denoted by $(\varepsilon_x^0, \varepsilon_\theta^0, \varepsilon_{x\theta}^0)$, $(N_x^0, N_\theta^0, N_{x\theta}^0)$ and $(N_x^{'}, N_\theta^{'}, N_{x\theta}^{'})$, respectively. The *x*-direction is parallel to the axis of the cylinder, the θ-direction is tangent to a circular arc, and the *z*-direction is normal to the median surface. Moreover, u_i, v_i, and w_i are the additional displacements due to buckling along *x*, θ, and *z*-directions, respectively. The total strains during buckling are given by [2]

$$\varepsilon_x = \varepsilon_x^0 + \frac{\partial u_i}{\partial x}, \quad \varepsilon_\theta = \varepsilon_\theta^0 + \frac{1}{R_i}\frac{\partial v_i}{\partial \theta} - \frac{w_i}{R_i},$$
$$\varepsilon_{x\theta} = \frac{1}{2}\left[\frac{1}{R_i}\frac{\partial u_i}{\partial \theta} + \frac{\partial v_i}{\partial x}\right], \tag{1}$$

where, R_i, u_i, v_i, and w_i (i = 1, 2, … , N) are the radius, and the additional deflections of the *i*th layer along the *x*, θ and *z*- directions, respectively. In the Eringen nonlocal elasticity model, the stress state at a reference point in the body is regarded to be dependent not only on the strain state at this point but also on the strain states at all of the points throughout the body. This model is based on the atomic theory of lattice dynamics and experimental observations on phonon dispersion [2] and [4]. For homogeneous and isotropic elastic solids, the constitutive equation of nonlocal elasticity can be written as [2]

$$(1 - e_0^2 a^2 \nabla_i^2)\sigma = C_O : \varepsilon, \tag{2}$$

where, the symbol ':' denotes the inner product of tensors with double contraction, C_0 is the elastic stiffness tensor of classical (local) isotropic elasticity, σ is the nonlocal stress tensor, ε is the strain tensor, e_0 is a material-dependent constant, and a is an internal characteristic length of the material (e.g., length of C-C bond or lattice spacing). In accordance with the thin shell assumption, the normal stress σ_z, the corresponding strain ε_z, and the shear strains ε_{xz} and $\varepsilon_{\theta z}$ are considered to be negligible. Consequently, the thin shell can be treated as a two-dimensional stress problem with $\partial\sigma_x/\partial\theta = \partial\sigma_\theta/\partial x = 0$. Considering the above assumptions, Eq. (2) can be written as [5] and [6]

$$\sigma_x - (e_0 a)^2 \frac{\partial^2 \sigma_x}{\partial x^2} = \frac{E}{1-\nu^2}(\varepsilon_x + \nu\varepsilon_\theta),$$
$$\sigma_\theta - (e_0 a)^2 \frac{1}{R_i^2}\frac{\partial^2 \sigma_\theta}{\partial \theta^2} = \frac{E}{1-\nu^2}(\varepsilon_\theta + \nu\varepsilon_x), \tag{3}$$

$$\sigma_{x\theta}-(e_0a)^2\left(\frac{\partial^2\sigma_{x\theta}}{\partial x^2}+\frac{1}{R_i^2}\frac{\partial^2\sigma_{x\theta}}{\partial\theta^2}\right)=\frac{E}{1+\nu}\varepsilon_{x\theta}.$$

The net forces are given by

$$N_x=\sigma_x h,\quad N_\theta=\sigma_\theta h\quad\text{and}\quad N_{x\theta}=\sigma_{x\theta}h.$$

Substituting Eqs. (1) and (3) into the above relations yields

$$\begin{aligned}
N_x &= K\left(\frac{\partial u_i}{\partial x}+\frac{\nu}{R_i}\frac{\partial v_i}{\partial\theta}-\nu\frac{w_i}{R_i}\right)+(e_0a)^2\frac{\partial^2 N_x}{\partial x^2}\\
&\quad+K(\varepsilon_x^0+\nu\varepsilon_\theta^0)=N_x'+N_x^0,\\
N_\theta &= K\left(\nu\frac{\partial u_i}{\partial x}+\frac{1}{R_i}\frac{\partial v_i}{\partial\theta}-\frac{w_i}{R_i}\right)+(e_0a)^2\frac{1}{R_i^2}\frac{\partial^2 N_\theta}{\partial\theta^2}\\
&\quad+K(\varepsilon_\theta^0+\nu\varepsilon_{\theta x}^0)=N_\theta'+N_\theta^0,\\
N_{x\theta} &= \frac{1}{2}K(1-\nu)\left(\frac{1}{R_i}\frac{\partial u_i}{\partial\theta}+\frac{\partial v_i}{\partial x}\right)+(e_0a)^2\\
&\quad\left(\frac{\partial^2 N_{x\theta}}{\partial x^2}+\frac{1}{R_i^2}\frac{\partial^2 N_{x\theta}}{\partial\theta^2}\right)+K(1-\nu)\varepsilon_{x\theta}^0=N_{x\theta}'+N_{x\theta}^0
\end{aligned},\tag{4}$$

where, $K=Eh/(1-\nu^2)$ is the effective extensional stiffness. Based on the classical thin shell theory [6] and [7], the governing equations for the elastic buckling of the MWNT can be derived as the following system of coupled equations:

$$\begin{aligned}
D\nabla_i^8 w_i &= \nabla_i^4 P_i(x,\theta)+N_x^0\frac{\partial^2}{\partial x^2}\nabla_i^4 w_i\\
&\quad+\frac{N_\theta^0}{R_i^2}\frac{\partial^2}{\partial\theta^2}\nabla_i^4 w_i+\frac{2N_{x\theta}^0}{R_i}\frac{\partial^2}{\partial x\partial\theta}\nabla_i^4 w_i\\
&\quad-(e_0a)^2\nabla_i^4\eta_i-\frac{Eh}{R_i^2}\frac{\partial^4 w_i}{\partial x^4},\ i=1,2,3,....,
\end{aligned}\tag{5}$$

where, $D=Eh^3/12(1-\nu^2)$ is the effective bending stiffness of the shell and η_i is defined as

$$\begin{aligned}
\eta_i &= \nabla_i^2 P_i+\frac{N_\theta^0}{R_i^4}\frac{\partial^4 w_i}{\partial\theta^4}+\frac{N_\theta^0}{R_i^2}\frac{\partial^4 w_i}{\partial x^2\partial\theta^2}\\
&\quad+N_x^0\frac{\partial^4 w_i}{\partial x^4}+\frac{4N_{x\theta}^0}{R_i^2}\frac{\partial^4 w_i}{\partial x^2\partial\theta^2}
\end{aligned},\tag{6}$$

where, P_i is the pressure exerted on the *i*th layer due to vdW interaction between the layers. It should be noted that the attractive vdW force is negative, the repulsive vdW force is positive, and the inward pressure is positive in Eq. (5). Thus, assuming infinitesimal buckling deflection between the two layers, the net pressure due to vdW interaction can be expressed by [8]

$$P_i(x,\theta)=-\sum_{j=1}^{i-1}\bar{P}_{ij}+\sum_{j=i+1}^{N}\bar{P}_{ij}+\Delta P_i(x,\theta),\tag{7a}$$

$$\Delta P_i=\sum_{j=1}^{N}\Delta P_{ij}=\sum_{j=1}^{N}c_{ij}(w_i-w_j)=w_i\sum_{j=1}^{N}c_{ij}-\sum_{j=1}^{N}c_{ij}w_j,\tag{7b}$$

$$\nabla_i^4 P_i=\nabla_i^4 w_i\sum_{j=1}^{N}c_{ij}-\sum_{j=1}^{N}c_{ij}\nabla_i^4 w_j,\tag{7c}$$

where, $\bar{P}_{ij}$ is the initial uniform vdW pressure contribution to the *i*th layer from the *j*th layer prior to buckling, *N* is the total number of layers of the multi-walled CNT, and $\Delta P_i(x,\theta)$ is the pressure increment after buckling. As only infinitesimal buckling is considered, $\Delta P_i(x,\theta)$ is assumed to be linearly proportional to the buckling deflection between the two layers, Eq. (7b). Finally, substituting the third of Eq. (7) into Eq. (5) gives

$$\begin{aligned}
D\nabla_i^8 w_i &= \nabla_i^4 w_i\sum_{j=1}^{N}c_{ij}+\sum_{j=1}^{N}c_{ij}\nabla_i^4 w_j+N_x^0\frac{\partial^2}{\partial x^2}\nabla_i^4 w_i\\
&\quad+\frac{N_\theta^0}{R_i^2}\frac{\partial^2}{\partial\theta^2}\nabla_i^4 w_i+\frac{2N_{x\theta}^0}{R_i}\frac{\partial^2}{\partial x\partial\theta}\nabla_i^4 w_i\\
&\quad-(e_0a)^2\nabla_i^4\eta_i-\frac{Eh}{R_i^2}\frac{\partial^4 w_i}{\partial x^4}.
\end{aligned}\tag{8}$$

2.2 vdW interaction relations

The vdW energy, due to the interatomic interaction, can be described by Lennard-Jones's potential pair method [9]. Assuming inward pressure to be positive, the initial pressure contribution P_{ij} caused by vdW interaction can be written as [8]

$$P_{ij}=\left[\frac{2048\varepsilon\sigma^{12}}{9a^4}\sum_{K=0}^{5}\frac{(-1)^K}{2k+1}\binom{5}{K}E_{ij}^{12}-\frac{1024\varepsilon\sigma^6}{9a^4}\sum_{K=0}^{2}\frac{(-1)^K}{2k+1}\binom{2}{K}E_{ij}^{6}\right]R_j.\tag{9}$$

The vdW interaction coefficients C_{ij} are determined from [8]

$$c_{ij}=-\left[\frac{1001\pi\varepsilon\sigma^{12}}{3a^4}E_{ij}^{13}-\frac{1120\pi\varepsilon\sigma^6}{9a^4}E_{ij}^{7}\right]R_j,\tag{10}$$

where, ε is the depth of the potential, σ is a parameter that is determined from the equilibrium distance, $a = 0.142nm$ is the C-C bond length, R_j is the radius of *j*th layer, and the subscripts *i* and *j* denote *i*th and *j*th layers, respectively. The area of each atom is equal to $9a^2/4\sqrt{3}$ [10]. The elliptic integrals E_{ij}^6, E_{ij}^7, E_{ij}^{12}, and E_{ij}^{13} are defined by [8]

$$E_{ij}^m = \frac{1}{(R_i + R_j)^m} \int_0^{\pi/2} \frac{d\theta}{\left[1 - \frac{4R_iR_j}{(R_i + R_j)^2}\cos^2\theta\right]^{m/2}}, \qquad (11)$$

where *m* is an integer. Eq. (10) gives the expression for the interaction coefficient c_{ij} that models vdW interaction after buckling in a multi-walled CNT. It should be noted that Eq. (10) was obtained by considering each tube as an individual continuum cylindrical shell.

2.3 Modeling the pressure

The net pressure due to vdW interaction from Eq. (7a) for the innermost and the outermost tubes are, respectively, given by

$$P_1 = -\overline{P}_{10} + \sum_{j=2}^{N} \overline{P}_{1j} + \Delta P_1,$$
$$P_N = -\sum_{j=1}^{N-1} \overline{P}_{ij} + \overline{P}_{N(N+1)} + \Delta P_N, \qquad (12)$$

where, $P_{\text{int}} = P_{10}$ is the applied internal pressure, and $P_{ext} = P_{N(N+1)}$ is the applied external pressure.

An initial interaction pressure between the outermost layer of the multi-walled carbon nanotube and its surrounding elastic medium, P_{ext}, can be written as [11] and [12]

$$P_{ext} = -d_N w_N, \qquad (13)$$

where, d_N is a spring constant which depends on the properties of the surrounding elastic medium [10]. The following relation has been proposed for d_N [12]:

$$d_N = \frac{E_m}{(1+v_m)R_N}, \qquad (14)$$

where, E_m, v_m, and R_N are the Young's module, the Poisson's ratio for surrounding elastic medium, and the radius of outermost layer, respectively. The effect of filling molecules in Eq. (12) can be modeled approximately by an internal pressure, P_{int}, representing an initial pressure between the innermost layer of the MWNT and its filling molecules. It is defined by

$$P_{\text{int}} = d_1 w_1. \qquad (15)$$

The spring constant d_1 in Eq. (15), which depends on the physical properties of the filling molecules and the innermost radius R_1 of the embedded MWNT, is given by [12]

$$d_1 = \frac{\beta E_f}{(1+v_f)R_1}, \qquad (16)$$

where, E_f, v_f and β are equivalent Young's modulus, the Poisson's ratio for filling molecules, and a constant coefficient that depends on the density and other physical properties of the filling molecules. In case there are no filling molecules inside the multi-walled carbon nanotube, P_{int} and β are set equal to zero.

3. Buckling analysis

Substituting Eq. (6) into Eq. (8), the following constitutive equation for the buckling of a multi-walled CNT for each layer is obtained:

$$\begin{aligned} D\nabla_i^8 w_i &= \nabla_i^4 w_i \sum_{j=1}^{N} c_{ij} - (e_0a)^2 \nabla_i^6 w_i \sum_{j=1}^{N} c_{ij} \\ &\quad - \sum_{j=1}^{N} c_{ij} \nabla_i^4 w_j + (e_0a)^2 \sum_{j=1}^{N} c_{ij} \nabla_i^6 w_j \\ &+ N_x^0 \left(\frac{\partial^2}{\partial x^2}\nabla_i^4 w_i - (e_0a)^2 \frac{\partial^4}{\partial x^4}\nabla_i^4 w_i\right) \\ &+ N_{x\theta}^0 \left(\frac{2}{R_i}\frac{\partial^2}{\partial x \partial \theta}\nabla_i^4 w_i - \left(\frac{2e_0a}{R_i}\right)^2 \frac{\partial^4}{\partial x^2 \partial \theta^2}\nabla_i^4 w_i\right) \\ &+ N_\theta^0 \left(\frac{1}{R_i^2}\frac{\partial^2}{\partial \theta^2}\nabla_i^4 w_i - \left(\frac{e_0a}{R_i}\right)^2 \frac{\partial^4}{\partial x^2 \partial \theta^2}\nabla_i^4 w_i \right. \\ &\left. - \left(\frac{e_0a}{R_i^2}\right)^2 \frac{\partial^4}{\partial \theta^4}\nabla_i^4 w_i\right) - \frac{Eh}{R_i^2}\frac{\partial^4 w_i}{\partial x^4} \end{aligned}, \qquad (17)$$

The buckling deflection of the *i*th layer is approximated by the following relation:

$$w_i = A_i \sin\left(\frac{m\pi}{L}x - n\theta\right), \qquad (18)$$

where, A_i (i =1, 2,...,N) are real constants, L is the

length of the MWNT, *m* is the axial half wave number, and *n* is the circumferential wave number. The net torque applied to the two ends of a multi-walled nanotube is

$$T = T_1 + T_2 + ... + T_N , \tag{19}$$

where, T_i *(i = 1,2,. . . ,N)* the torque exerted on the *i*th layer, and *T* is the net torque. Assuming that shear membrane forces in each layer of MWNTs are identical, the following relations can be written:

$$N^0_{x\theta 1} = N^0_{x\theta 2} = ... = N^0_{x\theta N} = \frac{T_1}{2\pi R_1^2} = \frac{T_2}{2\pi R_2^2} = ... = \frac{T_N}{2\pi R_N^2} \tag{20}$$

Based on the proportionality between the axial membrane forces and torque, the following relations are written [12] and [13]:

$$N^0_{xi} = \gamma N^0_{x\theta i} = \gamma N^0_{x\theta} = N^0_x \ , (i = 1,2,. . . ,N), \tag{21}$$

where, γ is the ratio of membrane axial force to shear forces. In a pre-buckling analysis, constraints for the ends of a cylindrical shell are usually neglected [5]. Thus, the normal equilibrium equations for each layer are given by

$$N^0_{\theta i} = N^0_\theta = P_i R_i , (i = 1,2,. . . ,N). \tag{22}$$

Substituting Eqs. (18), (21), and (22) into Eq. (17) yields the following set of algebraic equations for $w_1,....,w_i,.....,w_N$, for buckling modes, (*m* , *n*).

$$\begin{aligned}
&\{\{D\left[(\frac{m\pi}{L})^2 + (\frac{n}{R_i})^2\right]^2 - \sum_{j=1}^{N} c_{ij} \\
&-(e_0 a)^2\left[(\frac{m\pi}{L})^2 + (\frac{n}{R_i})^2\right]\sum_{j=1}^{N} c_{ij} \\
&+N^0_{x\theta}\left[\gamma(\frac{m\pi}{L})^2 + \gamma(e_0 a)^2(\frac{m\pi}{L})\right. \\
&\left.-\frac{2}{R_i}\frac{mn\pi}{L} + (\frac{2e_0 a}{R_i})^2(\frac{mn\pi}{L})^2\right] \\
&-P_i R_i\left[(\frac{n}{R_i})^2 + (\frac{e_0 a}{R_i})^2(\frac{mn\pi}{L})^2 + (e_0 a)^2(\frac{n}{R_i})^4\right] \\
&+\frac{Eh}{R_i^2}\left(\frac{1}{1+(\frac{Ln}{m\pi R_i})^2}\right)^2\}\}A_i \\
&+\{\{\left\{1+(e_0 a)^2\left[(\frac{m\pi}{L})^2 + (\frac{n}{R_i})^2\right]\right\}\sum_{j=1}^{N} c_{ij}\}\}A_j = 0.
\end{aligned} \tag{23}$$

If the net pressure($P_i = P_{i(i+1)} + P_{i(i-1)}$, $i, j = 1,2,.....,N$) exerted on the *i*th tube is assumed to be inward, Eq. (23) can be written in the following matrix form:

$$-N^0_{x\theta} X \begin{bmatrix} 1 & 0 & 0 & . & . & . & 0 \\ 0 & 1 & 0 & . & . & . & 0 \\ 0 & 0 & 1 & . & . & . & 0 \\ . & . & . & & & . & . \\ . & . & . & & & . & . \\ . & . & . & & & . & . \\ 0 & 0 & 0 & . & . & . & 1 \end{bmatrix} \begin{Bmatrix} A_1 \\ A_2 \\ A_3 \\ . \\ . \\ . \\ A_N \end{Bmatrix} =$$
$$Y \begin{bmatrix} b_{11} & c_{12} & c_{13} & . & . & . & c_{1N} \\ c_{21} & b_{22} & c_{23} & . & . & . & c_{2N} \\ c_{31} & c_{32} & b_{33} & . & . & . & c_{3N} \\ . & . & . & & & . & . \\ . & . & . & & & . & . \\ . & . & . & & & . & . \\ c_{N1} & c_{N2} & c_{N3} & . & . & . & b_{NN} \end{bmatrix} \begin{Bmatrix} A_1 \\ A_2 \\ A_3 \\ . \\ . \\ . \\ A_N \end{Bmatrix} , \tag{24}$$

or, equivalently,

$$\left[-N^0_{x\theta} X I_{N\times N} - Y C_{N\times N}\right] \begin{Bmatrix} A_1 \\ A_2 \\ . \\ . \\ . \\ A_N \end{Bmatrix} = 0, \tag{25}$$

where

$$X = \left[\gamma(\frac{m\pi}{L})^2 + \gamma(e_0 a)^2(\frac{m\pi}{L})^4 - \frac{2}{R_i}\frac{mn\pi}{L} + (\frac{2e_0 a}{R_i})^2(\frac{mn\pi}{L})\right],$$

$$Y = 1 + (e_0 a)^2\left[(\frac{m\pi}{L})^2 + (\frac{n}{R_i})^2\right],$$

$$I_{N\times N} = \begin{bmatrix} 1 & 0 & 0 & . & . & . & 0 \\ 0 & 1 & 0 & . & . & . & 0 \\ 0 & 0 & 1 & . & . & . & 0 \\ . & . & . & & & . & . \\ . & . & . & & & . & . \\ . & . & . & & & . & . \\ 0 & 0 & 0 & . & . & . & 1 \end{bmatrix},$$

$$C_{N\times N}=\begin{bmatrix} b_{11} & c_{12} & c_{13} & . & . & . & c_{1N} \\ c_{21} & b_{22} & c_{23} & . & . & . & c_{2N} \\ c_{31} & c_{32} & b_{33} & . & . & . & c_{3N} \\ . & . & . & & . & & . \\ . & . & . & & . & & . \\ . & . & . & & . & & . \\ c_{N1} & c_{N2} & c_{N3} & . & . & . & b_{NN} \end{bmatrix},$$

and

$$\begin{aligned} b_{ii} &= D\left[(\frac{m\pi}{L})^2+(\frac{n}{R_i})^2\right]^2-\sum_{j=1}^{N}c_{ij} \\ &-(e_0a)^2\left[(\frac{m\pi}{L})^2+(\frac{n}{R_i})^2\right]\sum_{j=1}^{N}c_{ij} \\ &-P_iR_i\left[(\frac{n}{R_i})^2+(\frac{e_0a}{R_i})^2(\frac{mn\pi}{L})^2+(e_0a)^2(\frac{n}{R_i})^4\right] \\ &+\frac{Eh}{R_i^2}\left(\frac{1}{1+(\frac{Ln}{m\pi R_i})^2}\right)^2 \end{aligned} \quad (26)$$

In order to obtain a non-trivial solution for Eq. (25), it is necessary to set the determinant of the coefficient matrix equal to zero

$$\det\left(Y[C]+N_{x\theta}^0X[I]\right)=0. \quad (27)$$

Solving Eq. (27) yields the buckling load of the MWNT for different wave numbers *m* and *n*. Eq. (27) determines the critical shear membrane force $N_{x\theta}^0(m,n)$ with a given axial force N_x^0 specified by the ratio γ. Thus, the critical torque on the MWNT, $T(m,n)$ is easily obtained from Eqs. (19) and (20), and hence the corresponding shear stress $\tau_{x\theta}(m,n)=N_{x\theta}^0(m,n)/h$.

To illustrate the influence of small length scale on the critical shear stress of an eleven-walled CNT, in accordance with Eq. (27), Ψ, i.e., the ratio of critical shear stress, is defined as:

$$\Psi=\frac{\tau_{x\theta}(e_0a=0)}{\tau_{x\theta}}. \quad (28)$$

4. Numerical results and discussion

4.1 The van der Waals interaction

4.1.1 The vdW interaction before buckling

To show vdW interaction prior to buckling, the pre-buckling vdW pressures between two adjacent layers are calculated by using Eq. (9) for an eleven-walled CNT with innermost radius in the range of $0.34-9.52nm$. The results are presented in Table 1. The value of P_{ij} in Table 1 represents the pressure contribution to the *i*th layer from the *j*th layer due to the vdW interaction before buckling. Note that the negative sign in Table 1 represents the attraction between the two layers. The effect of curvature on the vdW pressure is also shown in Table 1. For a tube with small radius (i.e., large curvature), the pre-buckling vdW pressure varies significantly and the effect of curvature becomes important. However, for a large radius (i.e., small curvature), the pressure variation is negligible. The pre-buckling pressures, due to the vdW interaction, approach constant values as the radius increases. The inward pressure is assumed to be positive. To show the dependence of all vdW pressures between two adjacent layers of an eleven-walled CNT on the radii of tubes, the pre-buckling pressure contributions to the *1st* and *11th* layers from one side layer and to the *2nd, 3rd, ...* layers from two side layers are presented in Fig. 3 for various innermost radii of the eleven-walled CNT. The vdW force exerted on each layer is due to all of the layers of the nanotube. The innermost layer is the first layer and the outermost layer is the eleventh layer. For any two adjacent layers, the pressure contribution to the outer tube from the inner tube is shown by solid lines in Fig. 3.

For small radii, the pressure contribution to the outer tube from the inner tube between any two adjacent layers drops sharply, whereas the pressure con-

Table 1. Pre-buckling pressure P_{ij} (Mpa) due to the vdW interaction for an eleven-walled CNT with various innermost radii R_1.

$R_1(nm)$	P_{61}	P_{62}	P_{63}	P_{64}	P_{65}	P_{67}	P_{68}	P_{69}	P_{610}	P_{611}
0.34	-0.1329	-0.4767	-2.2690	-19.0727	-665.8998	-768.7201	-25.5302	-3.5543	-0.8879	-0.3052
0.68	-0.1585	-0.5318	-2.4324	-19.8568	-677.8334	-757.7519	-24.8667	-3.4267	-0.8485	-0.2894
1.36	-0.1729	-0.5651	-2.5330	-20.3455	-685.3541	-750.7200	-24.4391	-3.3442	-0.8229	-0.2791
2.04	-0.1824	-0.5874	-2.6011	-20.6792	-690.5281	-745.8270	-24.1404	-3.2865	-0.8049	-0.2718
2.72	-0.1891	-0.6034	-2.6504	-20.9217	-694.3058	-742.2257	-23.9200	-3.2437	-0.7916	-0.2665
3.40	-0.1942	-0.6155	-2.6877	-21.1059	-697.1853	-739.4641	-23.7506	-3.2108	-0.7814	-0.2623
4.08	-0.1982	-0.6250	-2.7169	-21.2505	-699.4529	-737.2791	-23.6163	-3.1847	-0.7732	-0.2590
4.76	-0.2013	-0.6325	-2.7403	-21.3671	-701.2850	-735.5072	-23.5072	-3.1635	-0.7666	-0.2563
5.44	-0.2039	-0.6388	-2.7596	-21.4631	-702.7960	-734.0414	-23.4169	-3.1458	-0.7611	-0.2541
6.12	-0.2061	-0.6439	-2.7757	-21.5435	-704.0635	-732.8086	-23.3408	-3.1310	-0.7564	-0.2522
6.80	-0.2079	-0.6483	-2.7894	-21.6118	-705.1421	-731.7574	-23.2759	-3.1183	-0.7525	-0.2506
7.48	-0.2095	-0.6521	-2.8012	-21.6706	-706.0710	-730.8504	-23.2198	-3.1074	-0.7490	-0.2492
8.16	-0.2108	-0.6554	-2.8114	-21.7218	-706.8793	-730.0598	-23.1709	-3.0978	-0.7461	-0.2480
8.84	-0.2120	-0.6583	-2.8204	-21.7666	-707.5892	-729.3646	-23.1279	-3.0894	-0.7434	-0.2469
9.52	-0.2131	-0.6608	-2.8283	-21.8063	-708.2176	-728.7484	-23.0897	-3.0819	-0.7411	-0.2460

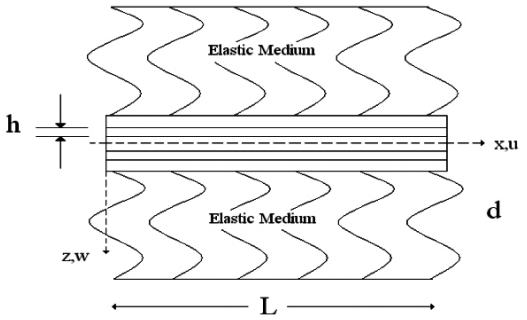

Fig. 2. Pressure exerted on an MWNT within an elastic medium characterized by a spring constant *d*.

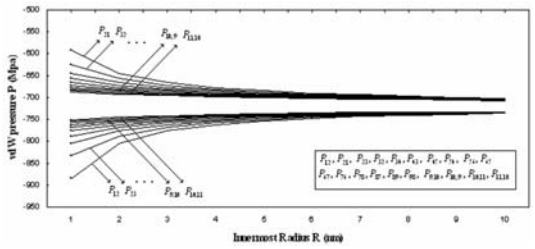

Fig. 3. Pre-buckling vdW pressure between two adjacent layers versus the innermost radius of an eleven-walled CNT.

tribution to the inner tube from the outer tube rises sharply with the increase of the radius. Therefore, a small radius significantly affects the pre-buckling vdW pressure. With increasing radius, the pressure tends to a constant value of -720 Mpa.

4.1.2 The vdW interaction after buckling

The vdW interaction coefficients, c_{ij} which are calculated from Eq. (10), are tabulated in Table 2 for an eleven-walled CNT with an innermost radius in the range of $0.34-9.52nm$. The coefficients c_{ij} in Table 2 represent the pressure increment contribution, due to vdW interaction after buckling, to layer *i* from layer *j*. It can be seen from the table that vdW interaction between two adjacent layers (e.g. c_{65} and c_{67}) is much larger than that of the two non-adjacent layers (e.g. c_{62} and c_{68}). It is also observed that the coefficient decreases rapidly by moving from the adjacent layer to the innermost or outermost layers. Thus, when the distance between the two layers is large enough, the value of the coefficient is very small and the vdW interaction can be neglected. It should be noted that the negative sign in Table 2 represents an attraction between the two layers, whereas the positive sign represents repulsion [8]. Interestingly, the absolute value of the coefficient c_{ij} increases with

Table 2. vdW interaction coefficient c_{ij} (Gpa/nm) for an eleven-walled CNT with various innermost radii R_1.

$R_1(nm)$	C_{61}	C_{62}	C_{63}	C_{64}	C_{65}	C_{67}	C_{68}	C_{69}	C_{610}	C_{611}
0.34	0.0045	0.0203	0.1292	1.6292	-92.7741	-107.1033	2.1821	0.2029	0.0380	0.0104
0.68	0.0054	0.0227	0.1388	1.6972	-94.4428	-105.5797	2.1260	0.1957	0.0363	0.0099
1.36	0.0059	0.0242	0.1447	1.7394	-95.4636	-104.6023	2.0897	0.1911	0.0353	0.0096
2.04	0.0062	0.0252	0.1486	1.7682	-96.2161	-103.9219	2.0643	0.1878	0.0345	0.0093
2.72	0.0065	0.0259	0.1515	1.7891	-96.7435	-103.4209	2.0456	0.1854	0.0339	0.0091
3.40	0.0067	0.0264	0.1536	1.8049	-97.1453	-103.0367	2.0312	0.1835	0.0335	0.0090
4.08	0.0068	0.0268	0.1553	1.8174	-97.4618	-102.7326	2.0197	0.1820	0.0332	0.0089
4.76	0.0069	0.0271	0.1566	1.8274	-97.7174	-102.4860	2.0105	0.1808	0.0329	0.0088
5.44	0.0070	0.0274	0.1577	1.8356	-97.9282	-102.2820	2.0028	0.1798	0.0326	0.0087
6.12	0.0071	0.0276	0.1587	1.8425	-98.1050	-102.1104	1.9963	0.1790	0.0324	0.0087
6.80	0.0071	0.0278	0.1597	1.8484	-98.2554	-101.9641	1.9907	0.1783	0.0323	0.0086
7.48	0.0072	0.0280	0.1601	1.8534	-98.3849	-101-8378	1.9860	0.1776	0.0321	0.0085
8.16	0.0072	0.0281	0.1607	1.8578	-98.4977	-101.7277	1.9818	0.1771	0.0320	0.0085
8.84	0.0073	0.0282	0.1612	1.8617	-98.5967	-101.6309	1.9781	0.1766	0.0319	0.0085
9.52	0.0073	0.0283	0.1617	1.8651	-98.6843	-101.5451	1.9749	0.1762	0.0318	0.0084

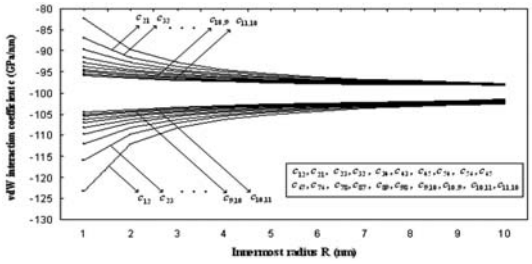

Fig. 4. vdW interaction coefficients between two adjacent layers versus the innermost radius of an eleven-walled CNT.

increasing the radius for $j<i$, while it decreases with increasing the radius for $j>i$. However, if the radius is large enough, the coefficient c_{ij} approaches a constant value which is independent of the curvature [14]. The relationships of the coefficients with the innermost radius of the eleven-walled CNT are plotted in Fig. 4. This implies that the vdW interaction coefficients are highly dependent on the radius for multi-walled CNTs with small radii. Large radii have little influence on the coefficients, as shown in Fig. 4. The coefficients approach a constant value of -100 (GPa/nm), which is close to the results reported by [3].

4.1.3 Buckling analysis

In this section, the buckling behavior of multi-walled carbon nanotubes is investigated by using the proposed vdW interaction model. The initial distance between two adjacent layers is assumed to be *h=0.34 nm*. The parameters used in the vdW interaction pressure in Eqs. (9) and (10) are taken to be $\varepsilon = 2.968meV$ and $\sigma = 0.34nm$ [10]. The effective

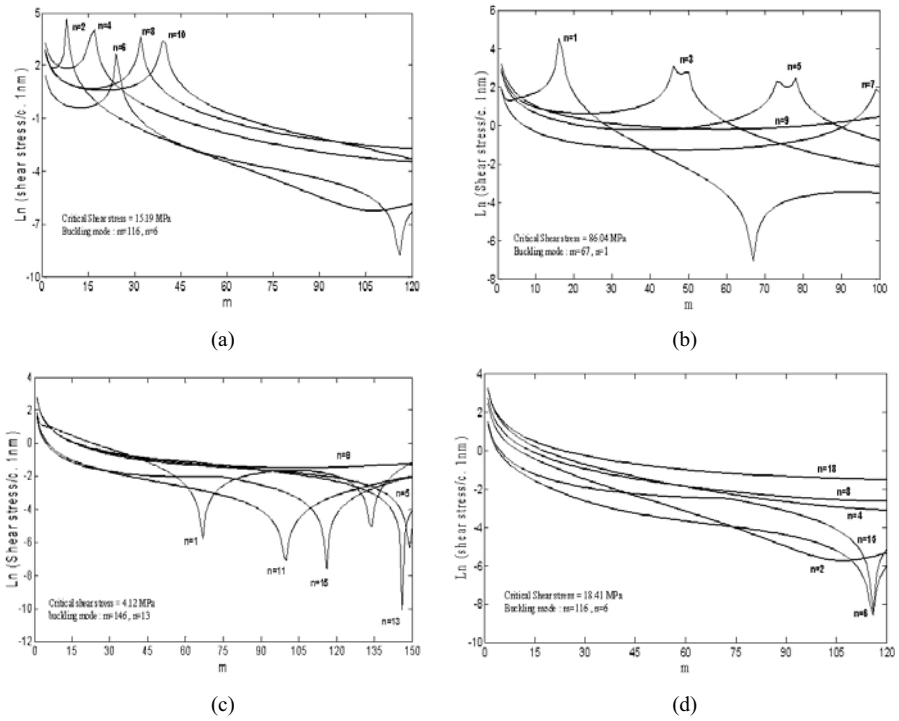

Fig. 5. Critical shear stress against the axial half wave number *m*, Example 1, combined torque and axial (a) tension $N_x^0 = 2N_{x\theta}^0$, (b) tension $N_x^0 = 0.5N_{x\theta}^0$, (c) tension $N_x^0 = 0.01N_{x\theta}^0$, (d) compression $N_x^0 = -1N_{x\theta}^0$, and lateral (internal and external) pressure.

bending stiffness *D=0.85 eV,* the effective in-plane stretching stiffness *Eh=360* J/m^2, Poisson's ratio $v = 0.3$, and the length $L = 12R_N$ (R_N is the outermost radius) are assumed for all the multi-walled CNTs considered in this study. For small length scale parameters *a=0.142 nm,* $e_0 = 0.82$ and for filling molecules $E_f = 2.5Gpa$, $v_f = 0.3$, and $\beta = 0.05$ are considered [2] and [12].

In this study, the MWNTs are divided into the following three categories based on the radius to thickness ratio:

(a) thin MWNTs (the innermost radius-to-thickness ratio is larger than five);

(b) thick MWNTs (the innermost radius-to-thickness ratio is around unity);

(c) (almost) solid MWNTs (the innermost radius-to-thickness ratio is smaller than 1/4).

Five different examples belonging to the above three categories, which are shown in Table 3, are considered in this study. Obviously, examples 1 and 2 belong to the thin MWNTs, examples 3 and 4 are thick MWNTs, while example 5 is a solid MWNT.

A significant result is that for all the three types of MWNTs, the buckling modes corresponding to the minimum critical shear stress for embedded MWNTs under combined torsional and axial loading and lateral (internal and external) pressure are clearly different from the modes for buckling under pure axial compression [3]. Moreover, they are different from the buckling modes under combined axial and torsional loading [12]. There exists a unique buckling mode, corresponding to the minimum critical shear stress for the values of *m* and *n*. Equation (27) determines the critical shear membrane force $N_{x\theta}^0(m,n)$. Tables 4 and 5 present the values of critical shear stress and the axial stress of an individual MWNT under combined loading for examples 1 and 3, respectively. The numerical results are presented in

Table 3. The geometrical data for MWNT samples.

Example The example number	Thin MWNTs		Thick MWNTs		Soild MWNTs
	1	2	3	4	5
$R_1(nm)$	8.5	18	2.7	6.5	0.65
R_1/Nt	5.00	6.62	0.99	1.20	0.24
$L(nm)$	118.32	244.56	60.96	139.20	36.36
N	5	8	8	16	8

R_1 is the innermost radius of an MWNT, N is the number of layers of the MWNT, and h(=0.34) is the effective thickness of an SWNTs.

Figs. 5 and 6. It is observed from these figures that the value of critical shear stress under combined torsional, axial and lateral loading is clearly dependent on the ratio of membrane axial force to shear force, axial loading direction (compression or tension), condition of filling molecules (internal pressure), and properties of the surrounding elastic medium (external pressure).

Table 4 . Value of m, n, τ_{cr} , σ_{cr} for example 1.

γ	m	n	τ_{cr} (MPa)	σ_{cr} (MPa)	Fig.
2	116	6	15.19	30.38	5a
0.5	67	1	86.04	43.02	5b
0.01	146	13	4.12	0.041	5c
-1	116	6	18.41	-18.41	5d

τ_{cr} is the critical shear stress, and σ_{cr} is the critical axial stress. Positive or negative denote the tension or compression of axial direction, respectively.

Table 5. Value of m, n, τ_{cr} , σ_{cr} for example 3.

γ	m	n	τ_{cr} (MPa)	σ_{cr} (MPa)	Fig.
2	137	5	1.75	3.50	6a
0.5	108	3	17.98	8.99	6b
0.01	61	9	15.85	0.158	6c
-1	137	5	2.81	-2.81	6d

The influence of small length scale on the critical shear stress for various buckling modes, shown in Fig. 7, can be obtained from Eq. (28). It can be observed that the effect of small length scale depends on the buckling modes. The effect of small length scale on the critical shear stress increases with an increase in the values of m and n .

4.1.4 The interlayer van der Waals interaction

To illustrate the interlayer vdW interaction effects (prior to buckling), the Lennard-Jones model is implemented. In a 7-walled CNT with innermost radius of 0.5 nm and gap of 0.34nm between every two adjacent layers, the effect of all layers on each other is investigated. The initial vdW pressure is calculated by using Eq. (9) for each layer of the 7-walled CNT. Table 6 shows the initial vdW pressure P_{ij} before buckling. The results show that the maximum vdW pressure occurs between the adjacent layers and specifically the innermost layer, i.e., P_{12} , and the minimum effect is between the first and the seventh layer,

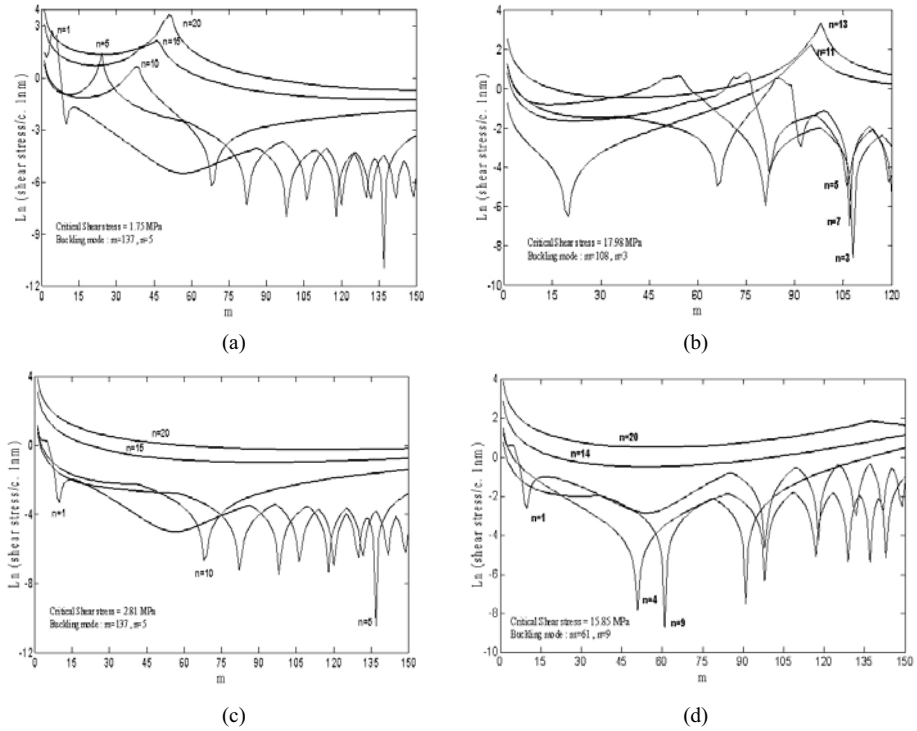

Fig. 6. Critical shear stress against the axial half wave number m, Example 3, combined torque and axial (a) tension $N_x^0 = 2N_{x\theta}^0$, (b) tension $N^0 = 0.5N_{x\theta}^0$, (c) tension $N^0 = 0.01N_{x\theta}^0$, (d) compression $N^0 = -1N_{x\theta}^0$, and lateral (internal and external) pressure.

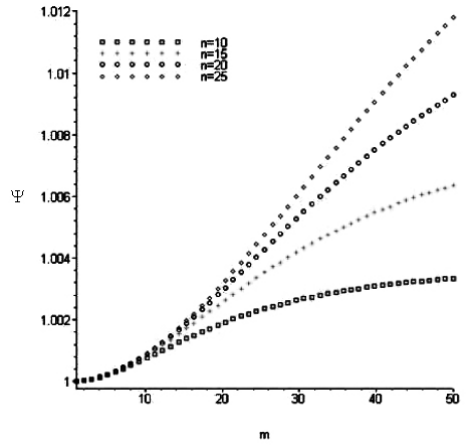

Fig. 7. Effect of small length scale on the critical shear stress for various buckling modes.

Table 6. Initial pressure P_{ij} (Mpa) due to vdW interaction between tubes i and j for a seven-walled CNT with innermost radius $R_{inner} = 0.5nm$.

Number of Layers,	$i=1$	$i=2$	$i=3$	$i=4$	$i=5$	$i=7$	$i=8$
$j=1$	0.0	-9.432	-0.358	-0.549	-0.0147	-0.0053	-0.0023
$j=2$	-5.614	0.0	-8.560	-0.307	-0.0454	-0.0119	-0.0042
$j=3$	-0.151	-6.093	-0.0	-8.177	-0.285	-0.0411	-0.011
$j=4$	-0.0181	-0.170	-6.350	0.0	-7.962	-0.2720	-0.040
$j=5$	-0.0039	-0.0205	-0.181	-6.510	0.0	-7.8240	-0.263
$j=6$	-0.0012	-0.0045	-0.022	-0.188	-6.620	0.0	-7.730
$j=7$	-0.00046	-0.0014	-0.005	-0.023	-0.193	-6.700	0.0

i.e., P_{17} . The initial vdW pressure between two adjacent layers is much larger than for the other two layers, and the vdW pressure decreases monotonically with increasing distance between two layers until it reaches zero or is negligible when the distance is large enough. Because of more interaction surface, the effect of each layer on its next layer is more than its previous one. The vdW pressure increases with an increase in the number of layers and their cross-section. Therefore, the critical load is more for larger MWNTs (considering constant internal radius).

5. Conclusions

Explicit formulas have been derived for critical shear and axial stresses for multi-walled carbon nanotubes under combined loading and lateral pressure taking into account the van der Waals interaction before and after buckling. The results have been obtained assuming a continuum cylindrical shell model and using the theory of nonlocal continuum mechanics. The results show that the internal pressure increases the critical load, while the external pressure tends to decrease the critical load. The buckling mode (*m,n*) corresponding to the critical shear stress of an embedded MWNT under combined loading is unique for all the eleven MWNTs considered with different values of the radius-to-thickness ratio. This is different from the case of these nanotubes under axial compression alone. The influence of small length scale on the critical shear stress of multi-walled carbon nanotubes under combined loading is discussed. The effect of small length scale on the critical shear stress depends on the buckling modes. The initial pressure between two adjacent layers is much larger than the other two layers.

Acknowledgments

The authors would like to thank the referees for their valuable comments, and also, the Iranian Nanotechnology Development Committee for their financial support.

References

[1] S. Iijima, Helical microtubes of graphitic carbon, *Nature* 354 (1991) 56-58.

[2] Y. Q. Zhang, G. R. Liu and X. Han, Effect of small length scale on elastic buckling of multi-walled carbon nanotube under radial pressure, *Phys. lett.* A349 (2006) 370-376.

[3] C. Y. Wang, C. Q. Ru and A. Mioduchowskil, Axially compressed buckling of pressured multi-walled carbon nanotubes, *Int. J. Solids Struct.* 40 (2003) 3893-3911.

[4] J. Yoon, C. Q. Ru and A. Mioduchowskil, Vibration of an embedded multiwall carbon nanotube, *Composite Sci. Technol.* 63 (2003) 1533-1545.

[5] S. P. Timoshenko and J. M. Gere, Theory of Elastic Stability, McGraw-Hill, New York (1961).

[6] Don. O. Brush and Bo. O. Almroth, Buckling of bars, plates, and shells, McGraw-Hill, New York (1975).

[7] L. H. Donnell, Beams, Plates, and Shells, McGraw–Hill, New York (1976).

[8] X. Q. He, S. Kitipornchai and K. M. Liew, Buckling analysis of multi-walled carbon nanotubes: a continuum model accounting for van der Waals interaction, *Int .J. Mech. Phys.* 53 (2005) 303-326.

[9] J. E. Lennard-Jones, The determination of molecular Fields: from the variation of the viscosity of a gas with temperature, Proc. Roy. Soc. 106A (1924) 441.

[10] R. Saito, G. Dresselhous and M. S. Dresselhous, Physical properties of carbon nanotubes, Imperial College press, London (1988).

[11] C. Q. Ru, Axially compressed buckling of a double-walled carbon nanotube embedded elastic medium, *J. Mech. Phys. Solids* 49 (2001) 1265-1279.

[12] X. Wang, Lu. Guoxing and Y. J. Lu, Buckling of embedded multi-walled carbon nanotubes under combined torsion and axial loading, *Int.J. Solid. Struct.* 44 (2007) 336-351.

[13] X. Wang, H. K. Yang and K. Dong, Torsional buckling of multi-walled carbon nanotubes, *Mater. Sci. Eng.* A 404 (2005) 314-322.

[14] O. Gulseren, T. Yildirim and S. Ciraci, Systematic ab initio study of curvature effects in carbon nanotubes, *Physical ReviewB* 65 (2002)153405.